Real-time measurements of cAMP production in live *Dictyostelium* cells

Anna Bagorda[1], Satarupa Das[1], Erin C. Rericha[2], David Chen[1], Jean Davidson[1] and Carole A. Parent[1,*]

[1]Laboratory of Cellular and Molecular Biology, Center for Cancer Research, National Cancer Institute, National Institutes of Health, Bethesda, MD 20892, USA
[2]Institute for Research in Electronics and Applied Physics, University of Maryland, College Park, MD 20740, USA
*Author for correspondence (parentc@mail.nih.gov)

Accepted 13 August 2009
Journal of Cell Science 122, 3907-3914 Published by The Company of Biologists 2009
doi:10.1242/jcs.051987

Summary

Cyclic AMP has a crucial role during the entire developmental program of the social amoebae *Dictyostelium*, acting both as an intracellular second messenger and, when secreted, as a directional cue that is relayed to neighboring cells during chemotaxis. Although significant knowledge about cAMP production in chemotaxing cells has been derived from studies performed on cell populations, cAMP dynamics at the single cell level have not been investigated. To examine this, we used a FRET-based cAMP sensor that possesses high cAMP sensitivity and great temporal resolution. We show the transient profile of cAMP accumulation in live *Dictyostelium* cells and establish that chemoattractants control intracellular cAMP dynamics by regulating synthesis via the adenylyl cyclase ACA. *aca*$^{-}$ cells show no significant change in FRET response following chemoattractant addition. Furthermore, cells lacking ACB, the other adenylyl cyclase expressed in chemotaxing cells, behave similarly to wild-type cells. We also establish that the RegA is the major phosphodiesterase that degrades intracellular cAMP in chemotaxis-competent cells. Interestingly, we failed to measure intracellular cAMP compartmentalization in actively chemotaxing cells. We conclude that cytosolic cAMP, which is destined to activate PKA, is regulated by ACA and RegA and does not compartmentalize during chemotaxis.

Supplementary material available online at
http://jcs.biologists.org/cgi/content/full/122/21/3907/DC1

Key words: Chemotaxis, cAMP, FRET, *Dictyostelium discoideum*

Introduction

The ubiquitous second messenger cAMP regulates a wide range of cellular processes, including differentiation, proliferation and cell motility. Cyclic AMP is also essential for the survival of the social amoebae *Dictyostelium discoideum* (Manahan et al., 2004). Upon starvation, these cells spontaneously aggregate and enter a developmental program that leads to the formation of a multicellular structure that can withstand harsh environmental conditions. A few hours after the initiation of starvation, cells start to synthesize cAMP and whereas part of the cAMP produced remains inside the cells to activate downstream effectors, part of the cAMP is secreted, functioning as a chemoattractant. The intracellular cAMP binds the regulatory subunit of PKA and releases its catalytic subunit, which regulates gene expression and is essential for development (Aubry and Firtel, 1999). Cells lacking the catalytic subunit of PKA fail to enter development (Anjard et al., 1993; Mann and Firtel, 1993). The secreted cAMP binds and stimulates specific G-protein-coupled receptors (named cARs for cAMP receptors), leading to the activation of a variety of effectors that control chemotaxis, gene expression and signal relay, via the synthesis and secretion of additional cAMP (Manahan et al., 2004).

Because cAMP is essential for the survival of *Dictyostelium*, its synthesis, degradation, and detection are exquisitely regulated. The synthesis of cAMP is mediated by adenylyl cyclases, which convert ATP into cAMP. *Dictyostelium* cells express distinct adenylyl cyclases during development (Kriebel and Parent, 2004). The enzyme responsible for cAMP production in early development is ACA (adenylyl cyclase expressed during aggregation), which is activated through cAR1 in a PI3K-dependent fashion. Cells lacking ACA fail to enter development and remain as smooth monolayers when starved (Pitt et al., 1992). We previously established that ACA is distributed in two distinct pools in polarized cells. One is restricted to the plasma membrane; the other is localized on highly dynamic intracellular vesicles that coalesce at the back of cells and is required for cells to migrate in a head-to-tail fashion and stream during chemotaxis (Kriebel et al., 2003; Kriebel et al., 2008). Another adenylyl cyclase expressed during aggregation is ACB (adenylyl cyclase B). In contrast to ACA, ACB appears to be constitutively active and is proposed to be required for terminal differentiation and is unresponsive to G-protein activation (Kim et al., 1998; Meima and Schaap, 1999; Anjard et al., 2001). Intracellular cAMP levels are also regulated by phosphodiesterases (PDEs), which degrade cAMP into 5′-adenosine monophosphate. *Dictyostelium* cells express four distinct PDEs with activity against intracellular cyclic nucleotides, with RegA (also referred to as PDE2) being the main high-affinity cAMP-specific PDE (Shaulsky et al., 1998; Bader et al., 2007). Cells lacking RegA behave similarly to cells lacking the regulatory subunit of PKA and exhibit constitutive PKA catalytic activity. Both cell lines show precocious development and aberrant terminal differentiation (Shaulsky et al., 1998).

Studies performed at the single cell level in *Dictyostelium* have shown the spatio-temporal dynamics of several chemotactic signaling components (Van Haastert and Devreotes, 2004; Bagorda et al., 2006). However, no studies have reported intracellular cAMP dynamics at the single cell level during chemotaxis. In the past few years the development of fluorescence resonance energy transfer (FRET)-based sensors has allowed the investigation of intracellular cAMP production in single live mammalian cells (Willoughby and Cooper, 2008). These types of studies have postulated new biological concepts, such as intracellular cAMP

compartmentalization in cardiac myocytes (Zaccolo and Pozzan, 2002) and waves of intracellular PKA activation in retinal neurons (Dunn et al., 2006). Based on these sensors, we have expressed a functional FRET-based cAMP probe in *Dictyostelium* cells. We aimed to determine (1) the intracellular cAMP dynamics following chemoattractant stimulation in single live *Dictyostelium* cells; (2) the specific contribution of ACA, ACB and RegA in this response; and (3) whether the distinct ACA distribution at the back of cells leads to a spatially restricted intracellular cAMP pool in chemotaxing cells.

Results

The expression of the tetrameric PKA-based cAMP sensor is downregulated during *Dictyostelium* development

The tetrameric PKA-based sensor is the first FRET probe developed to detect cAMP levels in live cells and it has been extensively used to monitor the intracellular cAMP dynamics in mammalian systems (Adams et al., 1991). It consisted of catalytic (C) and regulatory (R) subunits of PKA, chemically labeled with fluorescein and Rhodamine, respectively. In the absence of cAMP, both subunits form a tetrameric holoenzyme complex, R2C2, in which a high FRET signal between fluorescein and Rhodamine is observed. When cAMP binds to the regulatory subunits, the catalytic subunits dissociate, leading to a loss of FRET. Various modifications of this probe were later generated, where the donor came from the regulatory RII β-subunit of mammalian PKA tagged with CFP and the acceptor came from the catalytic subunit tagged with YFP (Fig. 1A) (Zaccolo and Pozzan, 2002). Here again, in the presence of low cAMP concentrations the probe retains its tetrameric structure and its FRET conformation. When cAMP levels increase and bind to the regulatory subunit, it dissociates from the catalytic subunit and the FRET signal is lost. To measure cAMP changes with this FRET-based sensor it is necessary to have the same level of expression of the donor and acceptor. We engineered the two constructs in *Dictyostelium* expression plasmids, co-transfected them in wild-type (WT) cells and assessed the expression level of the two plasmids using western analysis. During *Dictyostelium* development, a process during which cells express the various chemotactic signaling components and become polarized and motile, we observed a dramatic decrease in the expression levels of the CFP-RII β-subunit (Fig. 1B,C). We do not know why the CFP signal decreases during development. We speculate that overexpression of the active PKA catalytic subunit (the acceptor) downregulates the expression of the PKA regulatory subunit. Indeed, we observed that transfected cells were defective in development, because they were not able to form fully differentiated fruiting bodies (data not shown). Since the development of *Dictyostelium* is a PKA-dependent process, the lack of completion of the process suggests that PKA overexpression is altering the physiology of the cells. In any case, the uneven expression of the FRET acceptor and donor makes it impossible for us to use the tetrameric PKA sensor to detect intracellular cAMP dynamics in *Dictyostelium* cells.

The monomeric cAMP FRET sensor does not alter the development of *Dictyostelium* cells

We next constructed a FRET monomeric sensor based on the probe originally designed by Nikolaev and collaborators (Nikolaev et al., 2004). We cloned the cAMP-binding domain B from the mammalian PKA RII β-subunit between eCFP and eYFP in a *Dictyostelium*

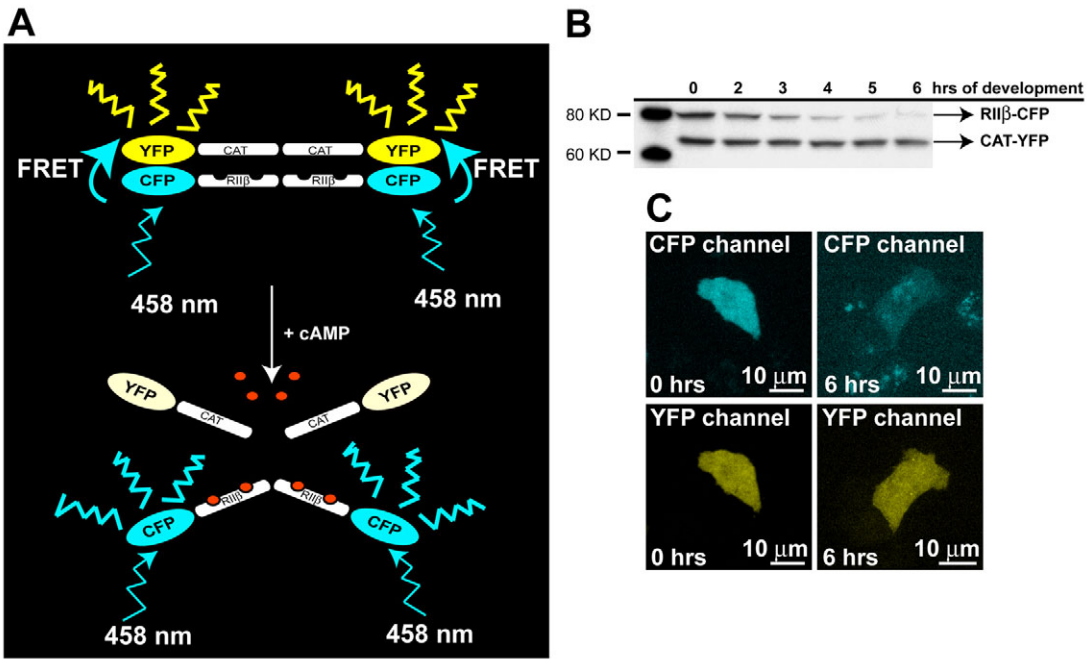

Fig. 1. The expression of the tetrameric PKA-based cAMP sensor is downregulated during *Dictyostelium* development. (A) Schematic representation of the PKA-based sensor: the RII β-subunit and catalytic subunit of mammalian PKA are respectively tagged with CFP and YFP. In the presence of low-cAMP concentrations, the PKA subunits retain a tetrameric conformation allowing FRET signal upon CFP excitation. When cAMP levels increase, cAMP binds the RII β-subunit causing a change in the PKA protein conformation, which results in the loss of FRET signal. (B) Western analysis of the expression of the PKA-based probe during *Dictyostelium* development. An anti-GFP antibody detects the expression level of the RIIβ-CFP and CAT-YFP in stable WT cells co-transfected with the two plasmids. The data are representative of three independent experiments. (C) Fluorescent images of CFP and YFP expression level of the PKA-based probe during *Dictyostelium* development. The data are representative of three independent experiments.

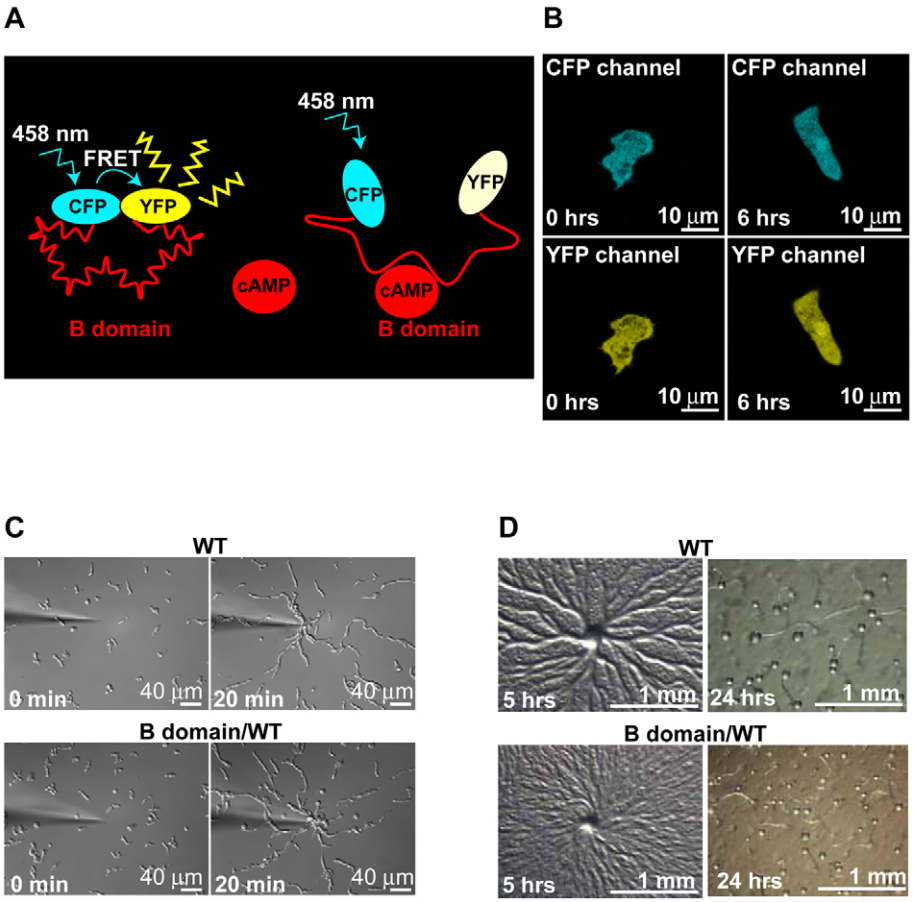

Fig. 2. The monomeric cAMP FRET sensor is expressed in *Dictyostelium* and does not compromise chemotaxis and development. (A) Schematic representation of the monomeric cAMP sensor: the cAMP-binding domain B from the mammalian PKA RII β-subunit is sandwiched between eCFP and eYFP. When cAMP levels are low, the probe retains a conformation that allows FRET signal upon CFP excitation. When cAMP levels increase and bind the B-domain, a change in the probe conformation ensues, which ultimately results in the loss of FRET signal. (B) Expression level of the B-domain sensor in WT *Dictyostelium* cells. Confocal images of the CFP and YFP signal of the monomeric cAMP sensor detected at 0 (left) and 6 hours (right) of development. The data are representative of six independent experiments. (C) Chemotaxis in a cAMP gradient. WT cells (upper panels) or WT cells expressing the B-domain probe (bottom panels) were developed for 5 hours, plated on a chambered coverslip and exposed to a micropipette filled with 10 μM cAMP. Images were taken just before and 20 minutes after the gradient was established. The data are representative of three independent experiments. (D) Development on a non-nutrient agar. WT cells (upper panels) or WT cells expressing the B-domain probe (bottom panels) were harvested from growth medium, extensively washed, resuspended in DB, plated on non-nutrient agar, and allowed to spontaneously develop. Numbers on the bottom left indicates hrs after plating. The data are representative of four independent experiments.

expression vector (see Materials and Methods for details). When cAMP levels are low, the probe retains a molecular conformation that allows FRET between the eCFP and eYFP (Fig. 2A). When cAMP levels increase and bind the B-domain, a conformational change of the probe ensues leading to a decrease of the FRET signal. The B-domain cAMP sensor, expressed in WT *Dictyostelium* cells, showed a uniform cytoplasmic distribution and a comparable level of the CFP and YFP signal (Fig. 2B). Since the probe binds cAMP, we worried that it might act as a sink for intracellular cAMP and alter development. We therefore carefully assessed the phenotype of cells expressing the B-domain. We first measured the ability of the cells to chemotax towards a point source of external cAMP. As shown in Fig. 2C, the cells transfected with the B-domain sensor were able to migrate directionally and align in a head to tail fashion during chemotaxis similarly to WT cells. In addition, we found that the transfected cells exhibited normal development when plated on non-nutrient agar showing characteristic aggregation streams and fruiting body formation (Fig. 2D). Taken together, these findings show that, in contrast to the tetrameric cAMP probe, the B-domain cAMP sensor is not toxic to cells, and is therefore a good method to study cAMP dynamics in *Dictyostelium*.

The monomeric cAMP FRET sensor responds to chemoattractant receptor stimulation

We next set out to visualize cAMP dynamics by measuring FRET efficiency changes in chemotaxis-competent cells. Confocal images were recorded as required by the acceptor-sensitized fluorescence technique and processed using the pFRET software (see Materials and Methods), which calculates FRET efficiency values. Fig. 3 shows a montage of images depicting the change in FRET signal observed as a function of time following a uniform saturating dose of chemoattractant (10 μM) in a representative cell (also see supplementary material Movie 1). The graph shows that upon receptor stimulation, there was a robust decrease in FRET efficiency (20.4±1.4%, n=10), which remained sustained during the 9 minute time course.

To determine whether the FRET efficiency decrease is specific for cAMP produced under receptor stimulation, we generated mutated versions of the B-domain probe lacking the ability to bind cAMP (supplementary material Fig. S1) (DiPilato et al., 2004; Lopez De Jesus et al., 2006). The two mutated versions of the B-domain probe were expressed to similar levels as the WT probe in WT cells and did not alter *Dictyostelium* development (data not shown). As depicted in Fig. 4A, chemoattractant stimulation of chemotaxis-competent cells transfected with either of the two mutated versions of the probe did not give rise to a change in FRET efficiency, strongly suggesting that the WT version of the FRET sensor specifically detects cAMP changes. To determine which AC pool the FRET efficiency decrease was specific for, we transfected the B-domain probe in *aca*$^-$ and *acb*$^-$ cells. We found that the decrease in FRET efficiency was highly specific for the cAMP produced by ACA, because *aca*$^-$ cells showed no significant decrease in FRET efficiency, whereas the *acb*$^-$ cells behave similarly to WT cells (Fig. 4B). These findings also establish that the large change in FRET response we observed in WT cells was not due to changes in cell shape. Indeed, *aca*$^-$ cells gave a normal cringe response when

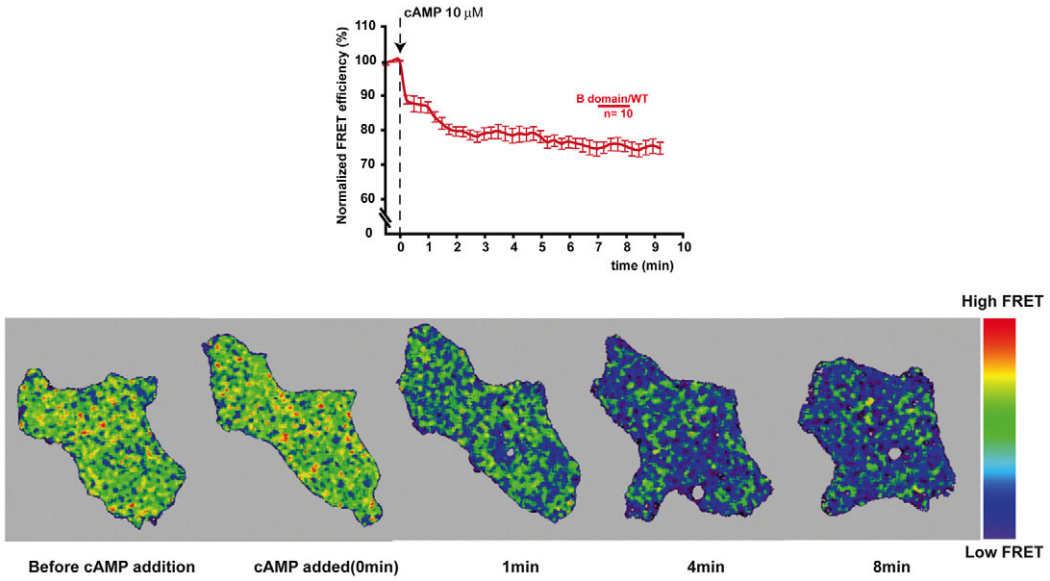

Fig. 3. The monomeric cAMP FRET sensor responds to chemoattractant receptor stimulation. Time course of the FRET efficiency average in single B-domain WT cells. Time points are 15 seconds apart and the saturating dose of cAMP is added at the third frame (dashed arrow). Mean ± s.e.m. values are presented. The images on the bottom were taken from a representative experiment (see supplementary material Movie 1) and show pseudocolor images of the FRET efficiency before and 1, 4 and 8 minutes after chemoattractant addition.

stimulated with chemoattractants, yet they showed no significant decrease in FRET efficiency. Together, these findings show that the B-domain cAMP probe specifically and robustly detects cAMP derived from ACA in chemotaxis-competent cells. Moreover, the results with *aca*⁻ cells clearly show that the FRET response is not affected by the exogenous cAMP stimulus nor does it respond to changes in intracellular cGMP levels, which occur normally in *aca*⁻ cells (Kuwayama and Van Haastert, 1998).

The monomeric cAMP FRET sensor is a highly sensitive probe

Fig. 3 shows that the intracellular levels of cAMP detected by the B-domain sensor are sustained during the entire time course of the experiment. This finding contrasts with previous biochemical studies, which show that once synthesized intracellular cAMP is rapidly cleared through intracellular degradation or secretion (Dinauer et al., 1980). We reasoned that the sustained FRET response observed under saturating stimulation conditions (10 μM) is dependent on the affinity of the B-domain probe for cAMP. A high-affinity probe would quickly saturate and not represent a true readout of the cAMP levels in cells. We therefore measured the affinity of the probe by performing in vitro fluorometric measurements of FRET responses on lysates from WT cells expressing the B-domain probe. This assay shows that the probe has an EC_{50} value <600 nM (Fig. 5A). To gain further insight into the ability of the probe to dissociate cAMP, we determined the capacity of the probe to return to its full FRET conformation upon the removal of cAMP. We found that the exogenous addition of the phosphodiesterase PdsA (Lacombe et al., 1986; Garcia et al., 2009) completely and rapidly reversed the loss of FRET caused by the addition 600 nM cAMP (Fig. 5B). These findings establish that the dissociation kinetic of our B-domain probe is fast enough to sense the rapid dynamic changes in intracellular cAMP.

Based on the estimation that intracellular cAMP levels can easily reach μM ranges (Roos et al., 1977), we concluded that our probe saturated rapidly, giving rise to a sustained FRET response. Indeed,

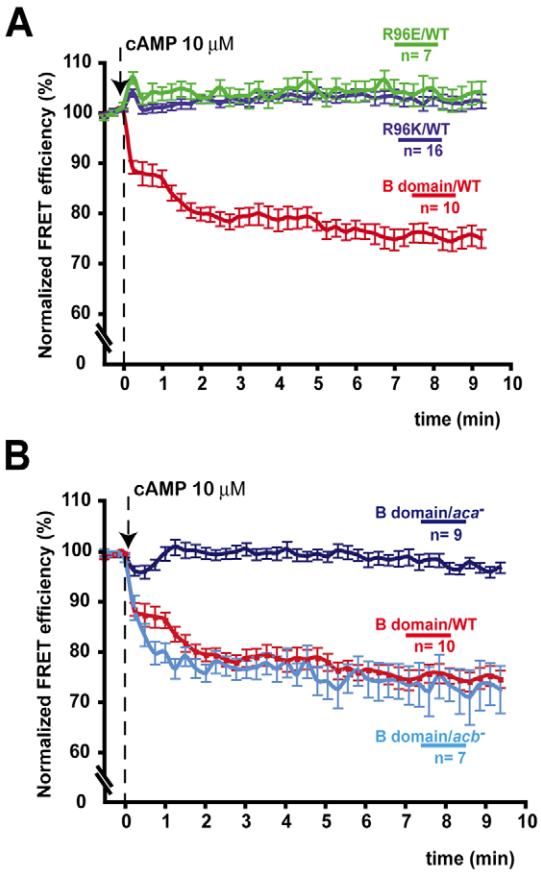

Fig. 4. The monomeric cAMP FRET sensor specifically detects cAMP derived from ACA. (A) Time course of the FRET efficiency average in WT cells transfected with non-binding mutants of the B-domain sensor (R96E; R96K). (B) Time course of the FRET efficiency average in WT, *aca*⁻ and *acb*⁻ cells expressing the B-domain sensor. The experiments were carried on as in Fig. 3. Mean ± s.e.m. values are presented.

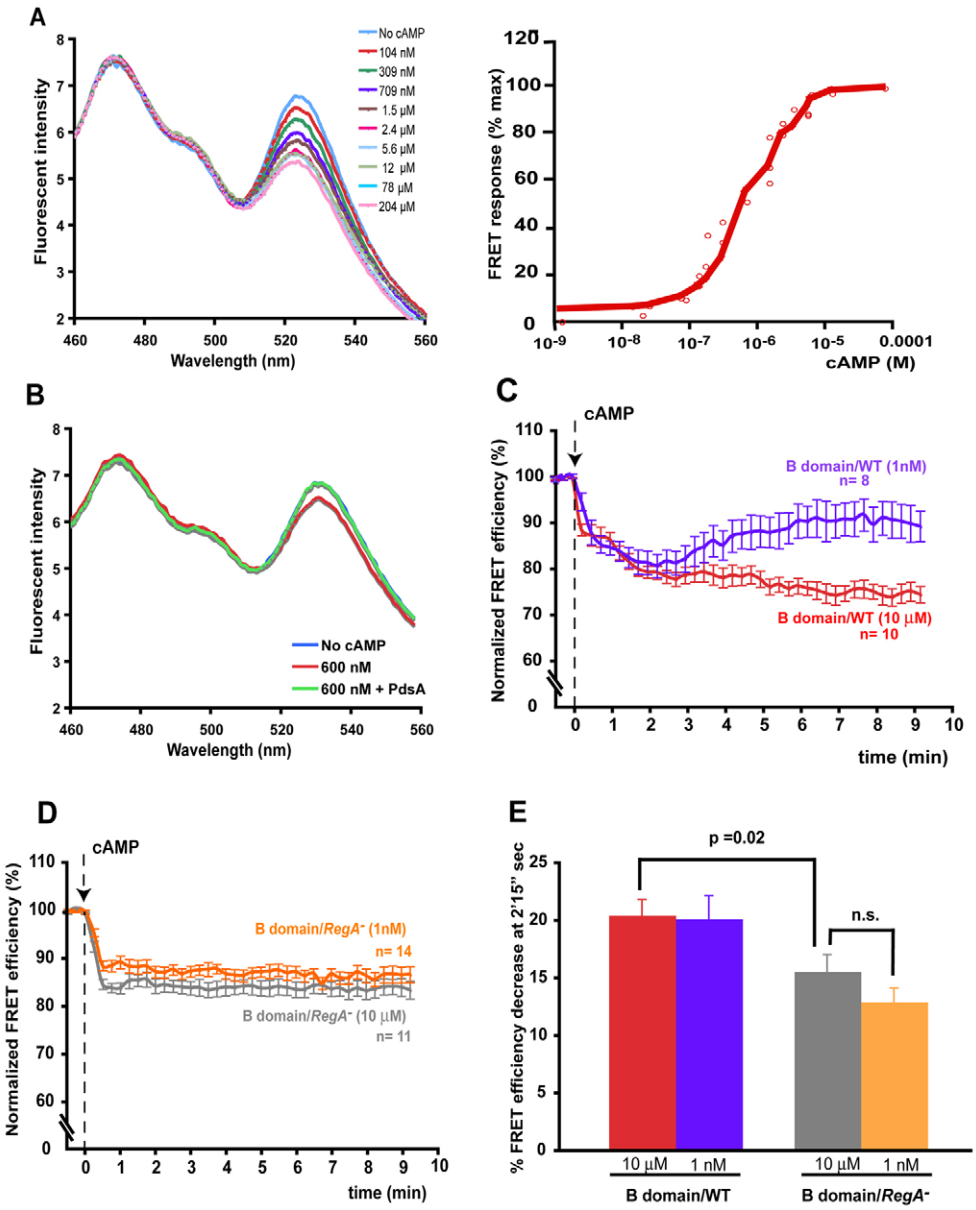

Fig. 5. The monomeric cAMP FRET sensor is a highly sensitive cAMP sensor. (A) cAMP dose-response curve of the B-domain sensor measured in vitro. Cell lysates obtained from B-domain WT cells were stimulated with various cAMP concentrations and the emission spectra under CFP excitation (425 nm) was measured with a spectrometer (left panel). The ratio between the CFP emission peak and the YFP emission peak derived from the spectrum measured for each cAMP concentration is represented as FRET response (right panel). The data are representative of three independent experiments. (B) FRET response in the presence of phosphodiesterase (PdsA). Cell lysates obtained from B-domain WT cells were stimulated with 600 nM cAMP in the presence or absence of PdsA and the emission spectra under CFP excitation (425 nm) was measured with a spectrometer as described in A. (C) Time course of the FRET efficiency average in B-domain WT cells stimulated with a subsaturating (1 nM; purple) or a saturating concentration of cAMP (10 µM; red). The experiments were carried on as described in Fig. 3. (D) Time course of the FRET efficiency average in B-domain *regA*$^{-}$ cells stimulated with subsaturating (1 nM; orange) or a saturating concentration of cAMP (10 µM; gray). The experiments were carried out as described in Fig. 3. (E) Summary of the percentage FRET efficiency decrease 2 minutes and 15 seconds after stimulation (the time where the peak cAMP accumulation occurs in B-domain WT cells stimulated with 1 nM cAMP). Mean ± s.e.m. values are presented.

when the cells were stimulated with a subsaturating dose of cAMP (1 nM) we observed a transient profile of cAMP accumulation, which reached a peak about 2-3 minutes after receptor stimulation and returned close to basal levels by 5-8 minutes (Fig. 5C). Based on previously published work, we attempted to generate a B-domain sensor with lower affinity for cAMP. Unfortunately, our efforts gave rise to a probe exhibiting an affinity that was too low (for details, see supplementary material Fig. S2). Taken together, our findings establish that the relative high affinity of our B-domain probe for cAMP allows the accurate detection of cAMP levels under subsaturating receptor stimulation conditions, in accordance with previously published biochemical measurements.

RegA is the major phosphodiesterase that degrades intracellular cAMP in chemotaxis-competent cells

To investigate the contribution of intracellular phosphodiesterase activity in the transient accumulation of cAMP we observed following subsaturating stimulation, we expressed the B-domain sensor in cells lacking RegA (Shaulsky et al., 1998; Bader et al., 2007). As shown in Fig. 5D, stimulation of these cells with either a saturating or a subsaturating concentration of chemoattractant, gave rise to a decrease in FRET efficiency that remained constant during the entire experimental time course. Moreover, when we compared the chemoattractant-mediated peak FRET response of WT and *regA*$^{-}$ cells, we found that the relative FRET decrease was lower in cells lacking RegA (Fig. 5E). We measured significantly lower basal raw FRET values in *regA*$^{-}$ cells compared with WT cells (18.6±0.5, n=25, versus 22.9±1.7, respectively; n=18; P=0.008), which could be due to higher basal cAMP levels in *regA*$^{-}$ cells. Nevertheless, because both degradation and secretion regulate intracellular cAMP levels, we were surprised to find that intracellular cAMP levels remain high for up to 10 minutes after a subsaturating stimulation with chemoattractants in *regA*$^{-}$ cells. This raised the possibility that *regA*$^{-}$ cells cannot secrete cAMP. To examine this further, we subjected chemotaxis-competent *regA*$^{-}$ cells to a micropipette

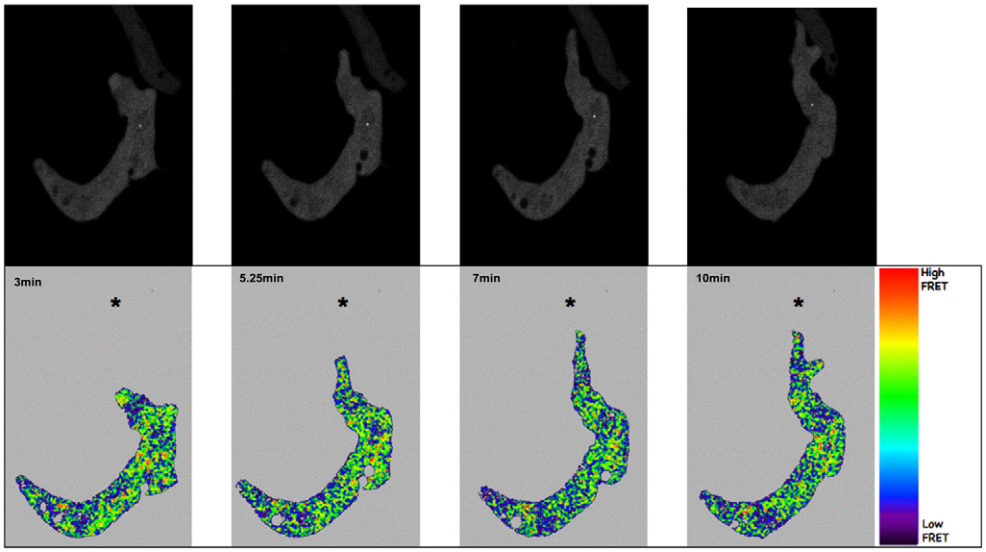

Fig. 6. cAMP dynamics in actively chemotaxing cells. A micropipette containing 10 μM cAMP is located at the top of the frames (indicated with an asterisk). The images were taken from a representative experiment (see supplementary material Movie 3) and show phase and pseudocolor images of the FRET efficiency at various time points.

filled with cAMP and monitored their ability to form stream during chemotaxis – a process that requires cAMP secretion (Kriebel et al., 2003). As depicted in supplementary material Movie 2, these cells responded to the micropipette by migrating towards its tip in a head-to-tail fashion to form streams. In contrast to WT cells, which formed long streams that resulted in large aggregation centers, *regA*$^{-}$ cells formed smaller aggregation centers and correspondingly shorter streams. We also used the EZ-Taxiscan chemotaxis chamber to assess chemotaxis and streaming. Using microfluidics, this system generates stable shallow chemoattractant gradients in a small, restricted area. Under these conditions, cells lacking RegA showed robust chemotaxis and signal relay as they readily formed streams during migration and aggregated into small clusters (see supplementary material Movie 3). Furthermore, as observed in WT cells, we found that ACA-YFP was enriched at the back of polarized *regA*$^{-}$ cells (data not shown). These findings establish that cells lacking RegA have the ability to secrete cAMP and relay signals to neighboring cells. It therefore appears that the transient intracellular cAMP accumulation observed under subsaturating conditions (measured by a return of FRET response to basal values) depends on the intracellular PDE activity of RegA.

The monomeric cAMP sensor does not reveal intracellular cAMP compartmentalization in actively chemotaxing cells

We next wanted to determine the spatio-temporal dynamics of intracellular cAMP in actively chemotaxing cells. We exposed chemotaxis-competent WT cells expressing the monomeric sensor to a micropipette filled with cAMP and monitored the FRET signal during chemotaxis. Fig. 6 depicts a montage of FRET images taken as cells are migrating (also see supplementary material Movie 4). Although we clearly observed variations in cytosolic cAMP levels in chemotaxing cells, careful analyses of the change in FRET efficiency in the migrating cells did not reveal intracellular compartmentalization of cAMP. Similarly, we did not observe compartmentalization in cells spontaneously migrating in streams (data not shown). From these findings, we conclude that the monomeric cAMP sensor does not reveal cAMP compartmentalization in cells chemotaxing to an external source of chemoattractant or in cells responding to natural cAMP waves.

Discussion

We aimed to measure intracellular cAMP dynamics in response to chemoattractant stimulation in *Dictyostelium* cells. Although cAMP has a crucial role throughout the developmental program of *Dictyostelium*, we focused on measuring cAMP fluctuations in single cells that were synchronized to the chemotaxis-competent stage. This allowed us to limit changes in responses that are dependent on aberrant development (particularly in mutant cell lines) and to focus on a homogenous cell population. Our findings establish that, following chemoattractant stimulation, the intracellular cAMP produced is synthesized by the adenylyl cyclase ACA and, as expected, the kinetics of the intracellular cAMP levels match the kinetics of ACA activation, which peak 1 minute after chemoattractant addition and slowly return to basal levels after ~5 minutes (Franca-Koh et al., 2006). Our findings also establish that the intracellular cAMP produced is degraded by the phosphodiesterase RegA. In cells lacking RegA, the cAMP produced following a subsaturating stimulation of chemoattractant does not decline and remains elevated. Using a different FRET probe that possesses a lower affinity for cAMP, the group of Satoshi Sawai reported similar transient cAMP fluctuations in WT cells (Gregor and Sawai, http://dictybase.org/DictyAnnualConference/dicty2007.pdf; Gregor, Fujimoto and Sawai, http://dictybase.org/DictyAnnualConference/dicty2008.pdf). Intriguingly, they also observed oscillations with ~3 minute period, under persistent chemoattractant stimulations. We have looked extensively for spatio-temporal changes in intracellular cAMP levels under a variety of conditions during chemotaxis and have not observed oscillatory fluctuations in intracellular cAMP levels using our probe. We suspect that the relatively lower affinity of their probe for cAMP (K_d=2 μM) allowed them to observe these oscillations.

Interestingly, it has been shown that, in chemotaxis-competent cells, intracellular cAMP is rapidly degraded and secreted (Dinauer et al., 1980). However, in *regA*$^{-}$ cells, cAMP levels remain high for up to 10 minutes after a subsaturating stimulation with chemoattractants. We have shown that these sustained intracellular cAMP levels are not due to the inability of *regA*$^{-}$ cells to secrete cAMP, because these cells can relay signals to neighboring cells, albeit abnormally. Indeed, Sawai and colleagues have shown that although *regA*$^{-}$ cells have the ability to propagate chemoattractant

waves, they do so less regularly and over shorter distances than seen in WT cells (Sawai et al., 2005). Although it is possible that the relative high affinity of our probe for cAMP does not allow us to measure a transient cAMP response in cells lacking RegA, we do not think that this is the case. First, although we measured higher basal cAMP levels in *regA*$^-$ cells, our probe retains a high basal FRET value in these cells that can further respond to cAMP fluxes. Second, in these cells the extent of ACA activation following a subsaturating stimulation gives rise to a small activity peak at 30 seconds, similarly to what we observe in WT cells (supplementary material Fig. S3). Nevertheless, in contrast to WT cells, we never measured a return to basal intracellular cAMP levels in the chemotaxis-competent *regA*$^-$ cells. To reconcile these findings, we propose that the two cellular pools of ACA generate two distinct pools of cAMP. In this scheme, the plasma-membrane-bound ACA would give rise to intracellular cAMP that is poised to activate PKA and is subject to degradation by RegA. Alternatively, the vesicular pool of ACA that is enriched at the back of cells (Kriebel et al., 2008) could produce cAMP that is destined for secretion and signal relay. Indeed, our probe is exclusively found in the cytoplasm of cells. Moreover, using electron microscopy, we have shown that the vesicular pool of ACA is mainly found in multivesicular bodies (MVBs) with the catalytic site of ACA facing the cytoplasmic side of the small vesicles released, which are called exosomes (Kriebel et al., 2008). Consequently, we propose that our monomeric cAMP FRET sensor solely detects the intracellular pool of cAMP synthesized from the plasma-membrane-bound ACA, which builds up in the absence of RegA, resulting in a prolonged FRET response. Our model would also explain why we do not measure cytosolic cAMP compartmentalization in chemotaxing and streaming cells. Since cells with aberrant intracellular cAMP dynamics, such as *regA*$^-$ and *pkareg*$^-$ cells, exhibit aberrant external cAMP wave propagation (Sawai et al., 2005), we envision that internal cAMP levels ultimately regulate cAMP secretion. This could occur via the cAMP effectors PKA or EPAC, similarly to that shown for various exocytosis events in mammalian cells (Szaszak et al., 2008). In particular, PKA has been shown to control the exocytosis of chemokine-containing storage granules in endothelial cells (Oynebraten et al., 2005). We foresee that compartmentalized ACA activity would exquisitely regulate differentiation and cell-cell communication events during starvation. Additional experiments are currently under way to specifically test this hypothesis.

Materials and Methods

FRET constructs and cell transfections

The RII β-CFP and the CAT-YFP plasmids were generated by amplification of the RII-CFP and C-YFP plasmids (Zaccolo and Pozzan, 2002). The amplification products were cloned into the unique *Bgl*II site of the *Dictyostelium* expression vector CV5, a p88d1-base plasmid with the Actin15/2H3 expression cassette (Johnson et al., 1991; Hughes et al., 1994), which provides stable protein expression throughout development (data not shown). The two plasmids were co-electroporated into *Dictyostelium* cells, as previously described (Howard et al., 1988), using a Bio-Rad gene pulser. Cells stably co-expressing the two plasmids were selected in medium containing 20 μg/ml G418. The DNA construct for the FRET B-domain sensor was generated through several cloning steps. First, the B-domain was obtained by PCR amplification of the mammalian cAMP-binding domain B (M264 to A403) using the RII-CFP plasmid as template and cloned into pCR 2.1 TOPO TA Cloning Vector (Invitrogen). Next the ECFP gene was amplified from Living Colors pECFP plasmid (BD Biosciences, NJ) and cloned at the 3′-end of the B-domain cDNA. The resulting B-domain-ECFP fusion was cloned into the pDXA-YFP-MCS1 vector (Knetsch et al., 2002) using the unique *Xho*I site, such that the YFP gene was at the 5′-end of the B-domain and finally cloned into the CV5 expression plasmid. Point mutations were introduced into the B-domain sensor construct using a QuikChange II XL-site-directed mutagenesis kit (Stratagene). The various expression plasmids have been deposited in the *Dictyostelium* Stock Center and are available publicly. Each sensor was electroporated in *Dictyostelium* cells and positive cells were selected in medium containing 20 μg/ml G418.

Cell culture and differentiation

WT (AX_3), B-domain WT, B-domain *aca*$^-$, B-domain *acb*$^-$ and B-domain *regA*$^-$ cells were grown in shaking cultures in HL5 medium, harvested by centrifugation, and differentiated to the chemotaxis-competent stage by resuspension in DB (5 mM Na_2PO_4, 5 mM NaH_2PO_4, pH 6.2, 2 mM $MgSO_4$, and 200 μM $CaCl_2$) and providing exogenous pulses of 75 nM cAMP as previously described (Kriebel et al., 2003).

Chemotaxis and development assays

Chemotaxis was measured by placing cells in a gradient of chemoattractant generated by a micropipette as previously described (Kriebel et al., 2003). The EZ-Taxiscan experiments were performed as described by the manufacturer on non-coated surfaces (Effector Cell Institute, Tokyo, Japan). Development on non-nutrient agar was performed as previously described (Devreotes et al., 1987). All images in a series were processed identically using IVision and/or Adobe Photoshop software.

Live cell FRET Imaging

A series of single-plane time-lapse images were collected with a Zeiss Axiovert 200M microscope fitted with the Zeiss LSCM 510 Meta confocal system (Carl Zeiss, Thornton NY), using a 63× Plan-Apochromat objective (Carl Zeiss). To measure FRET by the donor-sensitized acceptor fluorescence technique, three images were acquired for each set of measurements: (1) YFP fluorescence (514 nm excitation, 530 nm LP emission filter; (2) CFP fluorescence (458 nm excitation, 475-505 nm BP emission filter); (3) FRET (458 nm, 530 nm LP emission filter). The last is an uncorrected FRET image, which contains the 'bleed-through' of the CFP emission into the YFP detection channel and the cross-excitation of YFP by the CFP excitation laser. To obtain corrected FRET images, we acquired reference images from single-labeled CFP- and YFP-expressing cells (using the same set of acquisition parameters), as required by the pFRET Software (CircuSoft Instrumentation LLC, Hockessin, DE) that we subsequently used to analyze our FRET results (Wallrabe and Periasamy, 2005).

FRET analysis

By loading each Tiff file from every set of experiment in the pFRET software, we obtained FRET efficiency images and, for each of them, the average of FRET efficiency values. Those values were then normalized using, as reference value, the average of the three images preceding the stimulation. The reference value was then set to 100%.

In vitro FRET measurements

B-domain WT cells were starved for 2 hours in DB, centrifuged, washed twice and finally resuspended at 8×10^7 cells/ml in ice cold 10 mM Tris-HCl, pH 7.5, 0.2 mM EGTA, 200 mM sucrose. Cells were rapidly filter-lysed using 5 μm nucleopore filters. The resulting lysates were centrifuged at 9000 r.p.m. for 20 minutes at 4°C and the resulting supernatant used for analysis. Fluorescent emission spectra of total cell lysates from B-domain WT cells were measured (excitation 425 nm, emission range 460-550 nm) with a luminescence spectrometer (Aminco Bowman Series 2, Thermo Electron) before and after adding various concentration of cAMP. In a subset of experiments, partly purified PdsA (Garcia et al., 2009) was added immediately after stimulation with cAMP. The ratio of the CFP emission peak over YFP emission peak was calculated and expressed as a percentage of the maximum ratio, obtained with the saturating cAMP concentration.

We thank Manuela Zaccolo for providing the RII-CFP and C-YFP plasmids and the *Dictyostelium* Stock Center for providing the *acb*$^-$ and *regA*$^-$ cells. We also thank Michael Maurizi for allowing us to use his luminescence spectrometer and for his precious help to measure in vitro FRET as well as Alex Braiman and Valarie Barr for helping set up the in vivo FRET experiments and Gene Garcia for providing the partially purified PdsA. We would like to thank the Parent and Losert lab members as well as Paul Randazzo for excellent discussions and suggestions. This research was supported by the Intramural Research Program of the National Institutes of Health, National Cancer Institute, Center for Cancer Research. A.B. is a recipient of an Italian Cancer Federation Fellowship. E.C.R. is a recipient of a Career Award at the Scientific Interface from the Burroughs Wellcome fund. Deposited in PMC for release after 12 months.

References

Adams, S. R., Harootunian, A. T., Buechler, Y. J., Taylor, S. S. and Tsien, R. Y. (1991). Fluorescence ratio imaging of cyclic AMP in single cells. *Nature* **349**, 694-697.

Anjard, C., Etchebehere, L., Pinaud, S., Veron, M. and Reymond, C. D. (1993). An unusual catalytic subunit for the cAMP-dependent protein kinase of Dictyostelium discoideum. *Biochemistry* **32**, 9532-9538.

Anjard, C., Soderbom, F. and Loomis, W. F. (2001). Requirements for the adenylyl cyclases in the development of Dictyostelium. *Development* **128**, 3649-3654.

Aubry, L. and Firtel, R. A. (1999). Integration of signaling networds that regulate Dictyostelium differentiation. *Annu. Rev. Cell Dev. Biol.* **15**, 469-517.

Bader, S., Kortholt, A. and Van Haastert, P. J. (2007). Seven Dictyostelium discoideum phosphodiesterases degrade three pools of cAMP and cGMP. *Biochem. J.* **402**, 153-161.

Bagorda, A., Mihaylov, V. A. and Parent, C. A. (2006). Chemotaxis: moving forward and holding on to the past. *Thromb. Haemost.* **95**, 12-21.

Comer, F. I. and Parent, C.A. (2006). Phosphoinositide 3-kinase activity controls the chemoattractant-mediated activation and adaptation of adenylyl cyclase. *Mol. Biol. Cell.* **17**, 357-366.

Dao, K. K., Teigen, K., Kopperud, R., Hodneland, E., Schwede, F., Christensen, A. E., Martinez, A. and Doskeland, S. O. (2006). Epac1 and cAMP-dependent protein kinase holoenzyme have similar cAMP affinity, but their cAMP domains have distinct structural features and cyclic nucleotide recognition. *J. Biol. Chem.* **281**, 21500-21511.

Devreotes, P., Fontana, D., Klein, P. J., S. and Theibert, A. (1987). Transmembrane signaling in Dictyostelium. *Methods Cell Biol.* **28**, 299-331.

Dinauer, M. C., MacKay, S. A. and Devreotes, P. N. (1980). Cyclic 3′,5′-AMP relay in Dictyostelium discoideum III: the relationship of cAMP synthesis and secretion during the cAMP signaling response. *J. Cell Biol.* **86**, 537-544.

DiPilato, L. M., Cheng, X. and Zhang, J. (2004). Fluorescent indicators of cAMP and Epac activation reveal differential dynamics of cAMP signaling within discrete subcellular compartments. *Proc. Natl. Acad. Sci. USA* **101**, 16513-16518.

Dunn, T. A., Wang, C. T., Colicos, M. A., Zaccolo, M., DiPilato, L. M., Zhang, J., Tsien, R. Y. and Feller, M. B. (2006). Imaging of cAMP levels and protein kinase A activity reveals that retinal waves drive oscillations in second-messenger cascades. *J. Neurosci.* **26**, 12807-12815.

Franca-Koh, J., Kamimura, Y. and Devreotes, P. (2006). Navigating signaling networks: chemotaxis in Dictyostelium discoideum. *Curr. Opin. Genet. Dev.* **16**, 333-338.

Garcia, G. L., Rericha, E. C., Heger, C. D., Goldsmith, P. K. and Parent, C. A. (2009). The group migration of dictyostelium cells is regulated by extracellular chemoattractant degradation. *Mol. Biol. Cell* **20**, 3295-3304.

Howard, P. K., Ahern, K. G. and Firtel, R. A. (1988). Establishment of a transient expression system for Dictyostelium discoideum. *Nucleic Acids Res.* **16**, 2613-2623.

Hughes, J. E., Kiyosawa, H. and Welker, D. L. (1994). Plasmid maintenance functions encoded on Dictyostelium discoideum nuclear plasmid Ddp1. *Mol. Cell. Biol.* **14**, 6117-6124.

Johnson, R. L., Vaughan, R. A., Caterina, M. J., van Haastert, P. J. M. and Devreotes, P. N. (1991). Overexpression of the cAMP receptor 1 in growing Dictyostelium cells. *Biochemistry* **30**, 6982-6986.

Kim, H. J., Chang, W. T., Meima, M., Gross, J. D. and Schaap, P. (1998). A novel adenylyl cyclase detected in rapidly developing mutants of Dictyostelium. *J. Biol. Chem.* **273**, 30859-30862.

Knetsch, M. L., Tsiavaliaris, G., Zimmermann, S., Ruhl, U. and Manstein, D. J. (2002). Expression vectors for studying cytoskeletal proteins in Dictyostelium discoideum. *J. Muscle Res. Cell Motil.* **23**, 605-611.

Kriebel, P. W. and Parent, C. A. (2004). Adenylyl cyclase expression and regulation during the differentiation of Dictyostelium discoideum. *IUBMB Life* **56**, 541-546.

Kriebel, P. W., Barr, V. A. and Parent, C. A. (2003). Adenylyl Cyclase Localization Regulates Streaming during Chemotaxis. *Cell* **112**, 549-560.

Kriebel, P. W., Barr, V. A., Rericha, E. C., Zhang, G. and Parent, C. A. (2008). Collective cell migration requires vesicular trafficking for chemoattratant delivery at the trailing edge. *J. Cell Biol.* **183**, 949-961.

Kuwayama, H. and Van Haastert, P. J. (1998). Chemotactic and osmotic signals share a cGMP transduction pathway in Dictyostelium discoideum. *FEBS Lett.* **424**, 248-252.

Lacombe, M. L., Podgorski, G. J., Franke, J. and Kessin, R. H. (1986). Molecular cloning and developmental expression of the cyclic nucleotide phosphodiesterase gene of Dictyostelium discoideum. *J. Biol. Chem.* **261**, 16811-16817.

Lopez De Jesus, M., Stope, M. B., Oude Weernink, P. A., Mahlke, Y., Borgermann, C., Ananaba, V. N., Rimmbach, C., Rosskopf, D., Michel, M. C., Jakobs, K. H. et al. (2006). Cyclic AMP-dependent and Epac-mediated activation of R-Ras by G protein-coupled receptors leads to phospholipase D stimulation. *J. Biol. Chem.* **281**, 21837-21847.

Manahan, C. L., Iglesias, P. A., Long, Y. and Devreotes, P. N. (2004). Chemoattractant signaling in dictyostelium discoideum. *Annu. Rev. Cell Dev. Biol.* **20**, 223-253.

Mann, S. K. and Firtel, R. A. (1993). cAMP-dependent protein kinase differentially regulates prestalk and prespore differentiation during Dictyostelium development. *Development* **119**, 135-146.

Meima, M. E. and Schaap, P. (1999). Fingerprinting of adenylyl cyclase activities during Dictyostelium development indicates a dominant role for adenylyl cyclase B in terminal differentiation. *Dev. Biol.* **212**, 182-190.

Nikolaev, V. O., Bunemann, M., Hein, L., Hannawacker, A. and Lohse, M. J. (2004). Novel single chain cAMP sensors for receptor-induced signal propagation. *J. Biol. Chem.* **279**, 37215-37218.

Oynebraten, I., Barois, N., Hagelsteen, K., Johansen, F. E., Bakke, O. and Haraldsen, G. (2005). Characterization of a novel chemokine-containing storage granule in endothelial cells: evidence for preferential exocytosis mediated by protein kinase A and diacylglycerol. *J. Immunol.* **175**, 5358-5369.

Pitt, G. S., Milona, N., Borleis, J. A., Lin, K. C., Reed, R. R. and Devreotes, P. N. (1992). Structurally distinct and stage-specific adenylyl cyclase genes play different roles in Dictyostelium development. *Cell* **69**, 305-315.

Roos, W., Scheidegger, C. and Gerish, G. (1977). Adenylate cyclase activity oscillations as signals for cell aggregation in Dictyostelium discoideum. *Nature* **266**, 259-261.

Sawai, S., Thomason, P. A. and Cox, E. C. (2005). An autoregulatory circuit for long-range self-organization in Dictyostelium cell populations. *Nature* **433**, 323-326.

Shaulsky, G., Fuller, D. and Loomis, W. F. (1998). A cAMP-phosphodiesterase controls PKA-dependent differentiation. *Development* **125**, 691-699.

Szaszak, M., Christian, F., Rosenthal, W. and Klussmann, E. (2008). Compartmentalized cAMP signalling in regulated exocytic processes in non-neuronal cells. *Cell Signal.* **20**, 590-601.

Van Haastert, P. J. and Devreotes, P. N. (2004). Chemotaxis: signalling the way forward. *Nat. Rev. Mol. Cell Biol.* **5**, 626-634.

Wallrabe, H. and Periasamy, A. (2005). Imaging protein molecules using FRET and FLIM microscopy. *Curr. Opin. Biotechnol.* **16**, 19-27.

Willoughby, D. and Cooper, D. M. (2008). Live-cell imaging of cAMP dynamics. *Nat. Methods* **5**, 29-36.

Zaccolo, M. and Pozzan, T. (2002). Discrete microdomains with high concentration of cAMP in stimulated rat neonatal cardiac myocytes. *Science* **295**, 1711-1715.

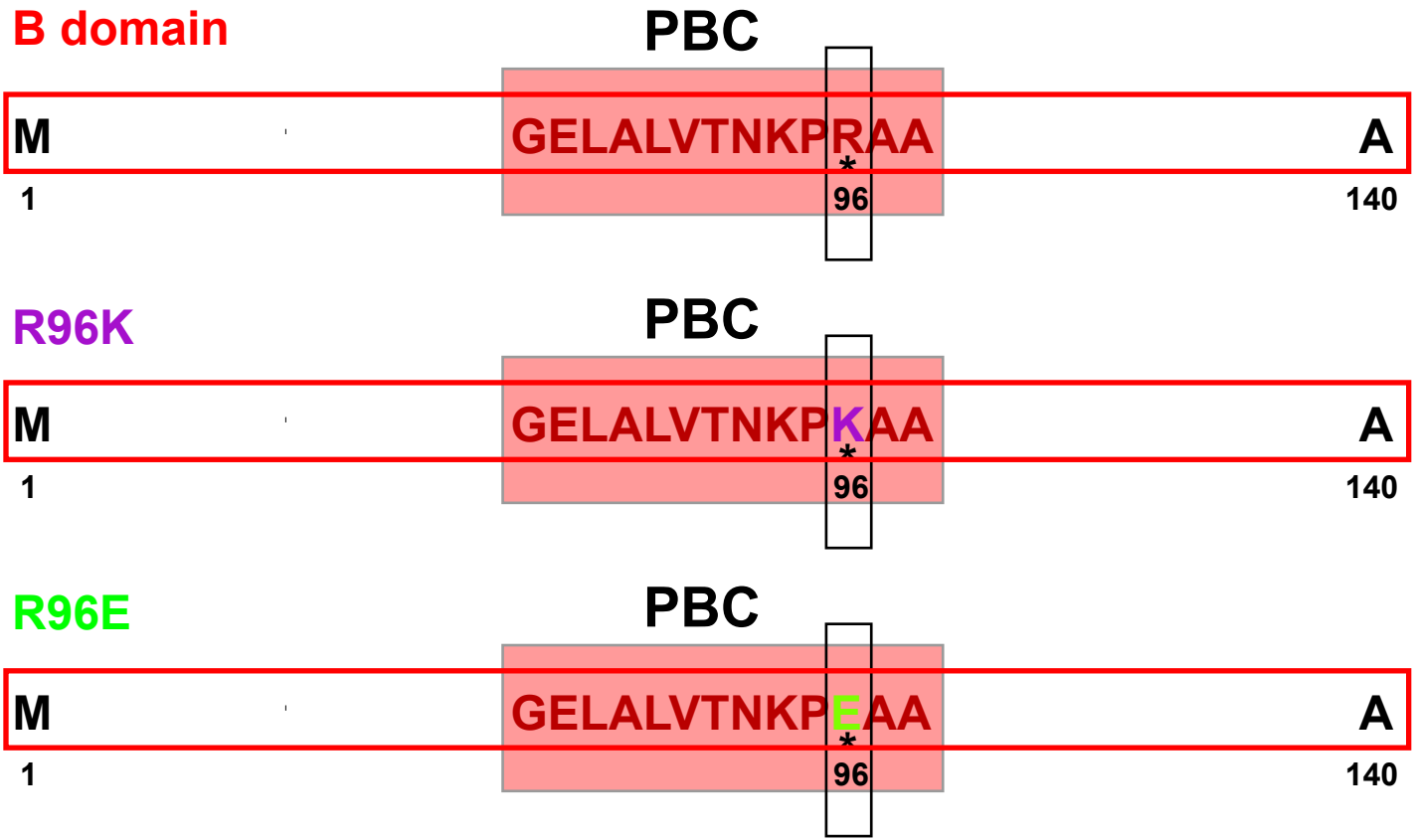
B domain
PBC
M
GELALVTNKPRAA
A
*
1
96
140
R96K
PBC
M
GELALVTNKPKAA
A
*
1
96
140
R96E
PBC
M
GELALVTNKPEAA
A
*
1
96
140

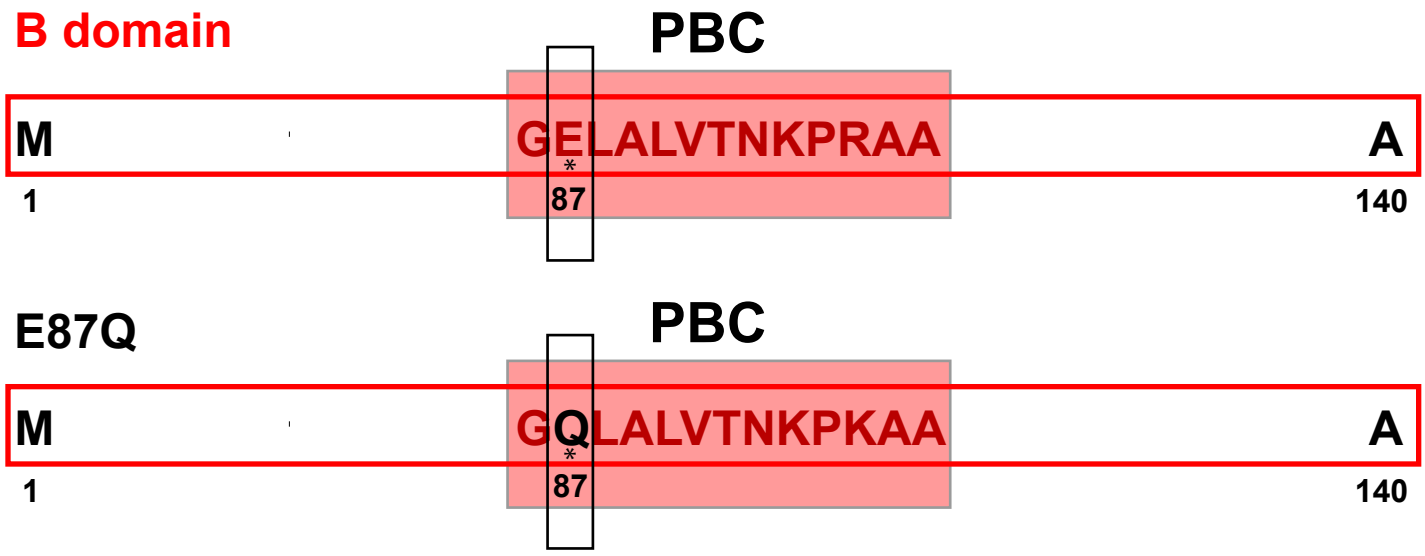
B domain
PBC
M
GELALVTNKPRAA
A
1
87
140
E87Q
PBC
M
GQLALVTNKPKAA
A
1
87
140

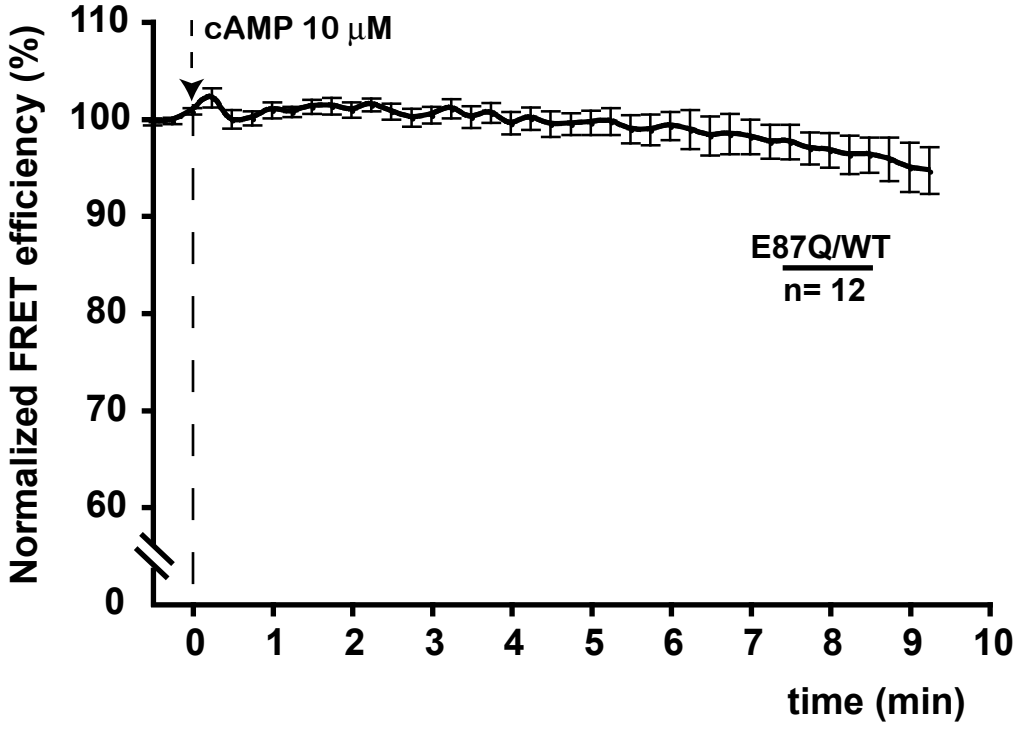
cAMP 10 μM
Normalized FRET efficiency (%)
110
100
90
80
70
60
0
E87Q/WT
n= 12
0
1
2
3
4
5
6
7
8
9
10
time (min)

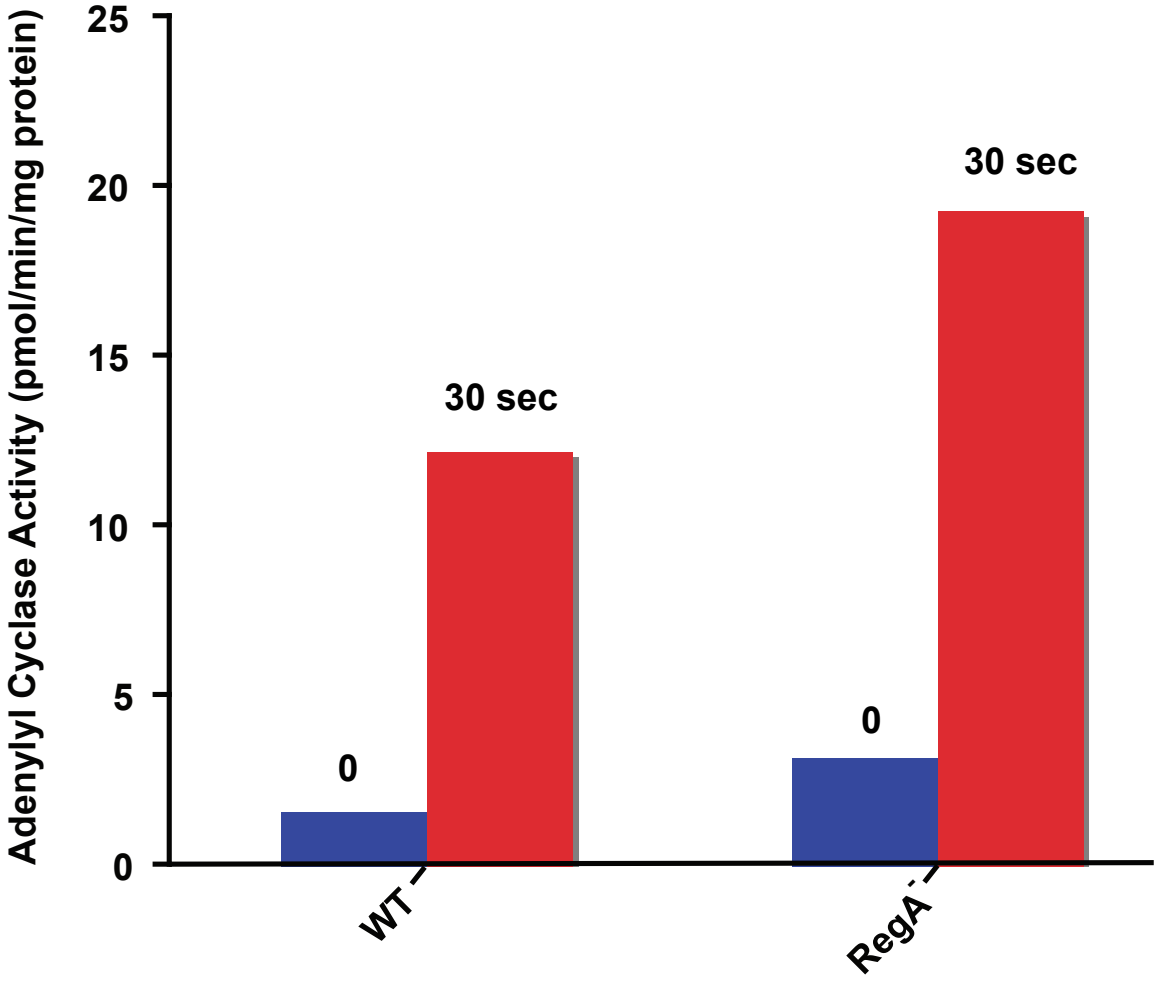
Adenylyl Cyclase Activity (pmol/min/mg protein)
25
20
15
10
5
0
30 sec
0
30 sec
0
WT
RegA-